Research

Author for correspondence:
Imran A. Rahman
e-mail: imran.rahman@oum.ox.ac.uk

A new ophiocistioid with soft-tissue preservation from the Silurian Herefordshire Lagerstätte, and the evolution of the holothurian body plan

Imran A. Rahman[1], Jeffrey R. Thompson[2,†], Derek E. G. Briggs[3], David J. Siveter[4], Derek J. Siveter[1,5] and Mark D. Sutton[6]

[1]Oxford University Museum of Natural History, Oxford OX1 3PW, UK
[2]Department of Earth Sciences, University of Southern California, Los Angeles, CA 90089-0740, USA
[3]Department of Geology and Geophysics and Yale Peabody Museum of Natural History, Yale University, New Haven, CT 06520-8109, USA
[4]School of Geography, Geology and the Environment, University of Leicester, Leicester LE1 7RH, UK
[5]Department of Earth Sciences, University of Oxford, South Parks Road, Oxford OX1 3AN, UK
[6]Department of Earth Sciences and Engineering, Imperial College London, London SW7 2BP, UK

IAR, 0000-0001-6598-6534; DEGB, 0000-0003-0649-6417; DeJS, 0000-0002-5305-2192

Reconstructing the evolutionary assembly of animal body plans is challenging when there are large morphological gaps between extant sister taxa, as in the case of echinozoans (echinoids and holothurians). However, the inclusion of extinct taxa can help bridge these gaps. Here we describe a new species of echinozoan, *Sollasina cthulhu*, from the Silurian Herefordshire Lagerstätte, UK. *Sollasina cthulhu* belongs to the ophiocistioids, an extinct group that shares characters with both echinoids and holothurians. Using physical–optical tomography and computer reconstruction, we visualize the internal anatomy of *S. cthulhu* in three dimensions, revealing inner soft tissues that we interpret as the ring canal, a key part of the water vascular system that was previously unknown in fossil echinozoans. Phylogenetic analyses strongly suggest that *Sollasina* and other ophiocistioids represent a paraphyletic group of stem holothurians, as previously hypothesized. This allows us to reconstruct the stepwise reduction of the skeleton during the assembly of the holothurian body plan, which may have been controlled by changes in the expression of biomineralization genes.

1. Introduction

Molecular data have proved crucial for reconstructing the phylogenetic relationships of major animal groups, greatly improving our understanding of metazoan evolution [1,2], but morphological data remain essential for reconstructing character evolution [3]. There are substantial morphological gaps between the body plans of many extant sister clades [4]; the fossil record can bridge these gaps, allowing us to reconstruct the stepwise evolution of crown-group body plans [5], but this undertaking is hampered where there is uncertainty about the phylogenetic placement of important taxa. Echinozoa, the subphylum of echinoderms that includes sea urchins (echinoids) and sea cucumbers (holothurians), provides a clear illustration of this problem. There is a conspicuous morphological gap between the body plans of extant echinoids and holothurians, and although there are extinct fossil forms that could fill this gap, their phylogenetic positions are uncertain [6–8]. As a result, the pattern of evolution of echinoid and holothurian body plans and the nature of their most recent common ancestor remain unclear.

Here we describe a new species of Silurian echinozoan, *Sollasina cthulhu*, from the Wenlock Series (approx. 430 Ma) Herefordshire Lagerstätte of the UK [9,10]. *Sollasina* belongs to the extinct Ophiocistioidea, an echinozoan

group characterized by a complex jaw apparatus, long plated tube feet and a body-wall skeleton either composed entirely of large plates or mostly reduced to small spicules [11–13]. Thus, ophiocistioids combine characteristics of echinoids (e.g. complex jaw apparatus) and holothurians (e.g. body-wall skeleton mostly reduced to small spicules), and can potentially inform reconstructions of character evolution in these groups.

An exceptionally well-preserved fossil specimen was studied using physical–optical tomography (sensu [14]) and computer reconstruction, revealing internal soft tissues in an ophiocistioid for the first time. Our detailed morphological description informed phylogenetic analyses which strongly support the placement of ophiocistioids as stem holothurians. This has important implications for the evolutionary assembly of the holothurian body plan.

2. Material and methods

Thirteen specimens of the new ophiocistioid are known, all from the single known locality of the Herefordshire Lagerstätte. Like other fossils from this Lagerstätte, specimens are preserved three-dimensionally as calcite void-fill in calcareous concretions [15]. One exceptionally well-preserved specimen was selected for detailed study by physical–optical tomography [14]. The specimen was cut into seven pieces, serially ground at 30 μm intervals, and the exposed surfaces were imaged using a Leica digital camera attached to a Wild binocular microscope. The resulting sets of slice images were digitally reconstructed as a three-dimensional (3-D) virtual model using the SPIERS software suite [16]. Datasets from serial grinding and the final 3-D model in VAXML/STL format are housed at the Oxford University Museum of Natural History (OUMNH) and are also available from the Dryad Digital Repository: https://doi.org/10.5061/dryad.c71qf48 [17].

We undertook parsimony and Bayesian phylogenetic analyses to establish the phylogenetic position of the new ophiocistioid. Our character matrix was modified from that of Smith & Reich [18], and supplemented with six extant echinoid genera (Asthenosoma, Diadema, Echinocardium, Encope, Eucidaris, Strongylocentrotus) and five additional fossil echinozoan genera (Bothriocidaris, Bromidechinus, Eothuria, Neobothriocidaris, Unibothriocidaris). The resulting matrix consists of 26 taxa and 51 characters (electronic supplementary material, table S1, data S1). Parsimony analyses were run in PAUP* v. 4.0 [19] using a heuristic search with 10 000 random addition sequence replicates using starting trees obtained by stepwise addition and branch swapping through tree bisection and reconnection. The somasteroid Archegonaster was used as an outgroup. Bayesian analyses were run in MRBAYES v. 3.2 [20] using the Mkv model of character change [21]. Rate variation was modelled using a gamma distribution with a prior of exponential(1.0), and branch lengths were unconstrained with a compound Dirichlet prior [22]. The joint posterior distribution of tree topologies, branch lengths and model parameters were estimated with Markov chain Monte Carlo, using four chains with two runs for each chain. Each chain was run for 12 000 000 generations, sampling every 1000 generations. Analyses were run until the average deviation of split frequencies was below 0.01. The first 25% of samples were discarded as burn-in.

3. Systematic palaeontology

Phylum: Echinodermata [23] (ex [24])
Class: Ophiocistioidea [25]
Family: Sollasinidae [26]

Genus: Sollasina [26]
Type species: Eucladia woodwardi Sollas, 1899, by original designation of Fedotov, 1926; from the Ludlow Series, Silurian, of Church Hill, Leintwardine, Herefordshire, UK.
Other species: Sollasina cthulhu sp. nov.

(a) Diagnosis of genus

Sollasinidae with relatively small jaw apparatus; two columns of four adradial plates each and nine plated tube feet per ambulacral area; plates of non-peristomial tube feet arranged in longitudinal rows; aboral thecal plates with strong granular ornamentation. (Amended from [6,11]).

(b) New species

Sollasina cthulhu sp. nov.
urn:lsid:zoobank.org:act: 4480289B-574C-4F7A-92F7-692DB 3045B9E.

(c) Etymology

Named for the Cthulhu mythos of H. P. Lovecraft [27], a fictional universe populated with bizarre tentacled monsters. Pronunciation: kuh-THOO-loo.

(d) Material

Holotype: OUMNH C.29662, an almost complete specimen reconstructed as a virtual fossil. Other (unground) specimens: OUMNH C.29648, C.36006, C.36013, C.36064–C.36072.

(e) Locality and horizon

Herefordshire, UK; upper part of the Wenlock Series, Silurian.

(f) Diagnosis of species

Sollasina with pentagonal theca; one column of six perradial plates per ambulacral area; four or five plates per interambulacral area.

(g) Description

The theca is approximately 15 mm in diameter and pentagonal in outline, with thin, imbricate plates (figure 1a,c). The oral (lower) surface is slightly concave; the aboral (upper) surface is partly collapsed, but was presumably convex in life. The oral surface of the theca consists of five wide ambulacral areas, composed of columns of perradial and adradial plates, which alternate with five narrow interambulacral areas (figure 1a,k). The aboral surface of the theca consists of numerous irregularly arranged plates (figure 1c).

The peristome occupies the middle of the oral surface (figure 1a,g). It is subcircular in outline and approximately 6 mm in diameter. Five thick, rhomboidal, interradially-positioned plates form the jaw apparatus, which occupies about half the peristome diameter (figure 1a,g). Details of the jaw plates and the nature of any plating surrounding the jaw apparatus are unclear. The madreporite is located within an interambulacrum on a plate between adjacent adradial plates and the peristome; it is approximately 1.1 mm in diameter, dome-shaped, with a circle of small pores at the summit (figure 1g,h). Adjacent to the madreporite, on the same plate, there is a rounded protuberance with a single pore at the summit, which probably represents a gonopore
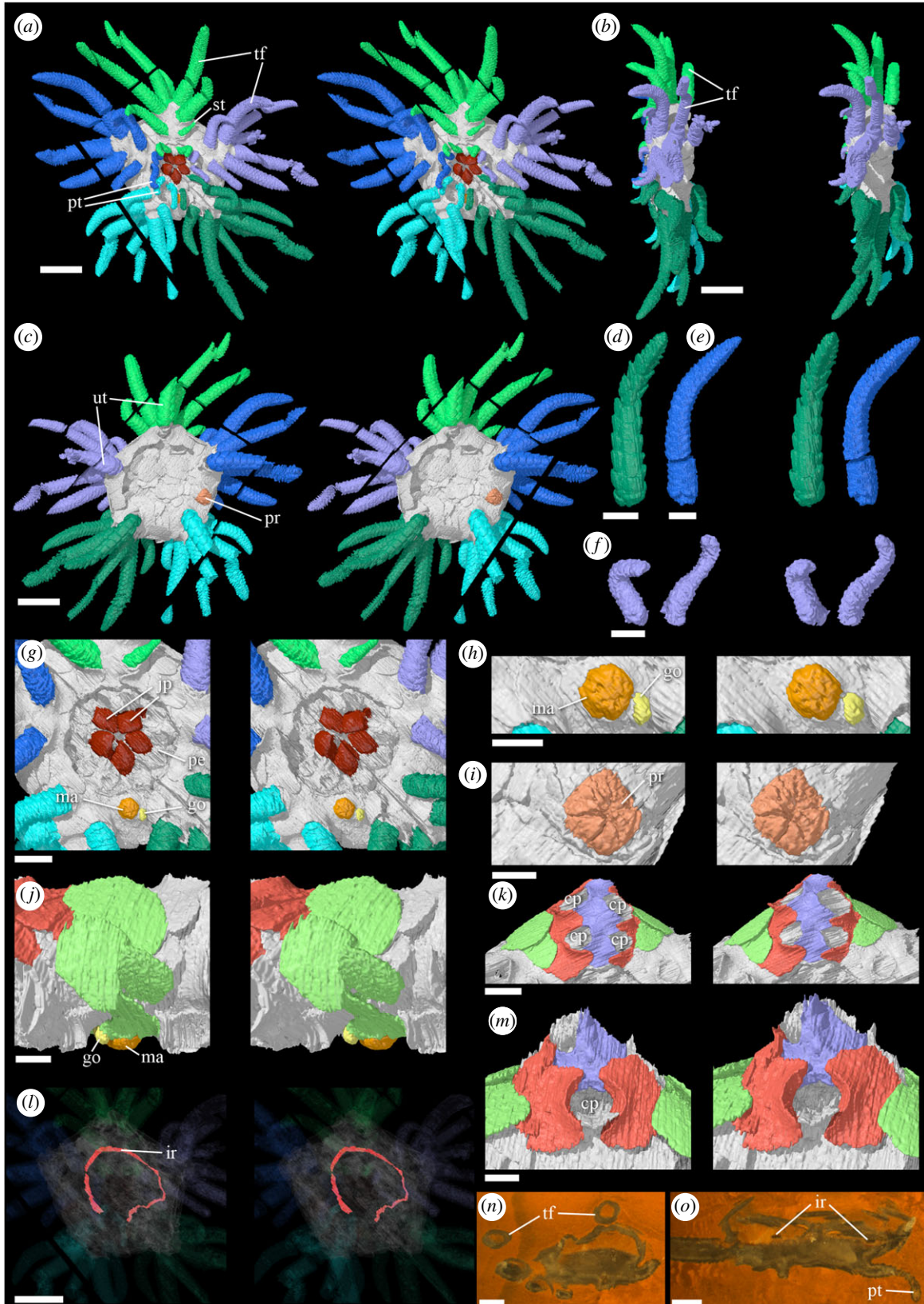
3

Figure 1. *Sollasina cthulhu* (OUMNH C.29662). (*a–m*) Virtual reconstructions (stereo-pairs), (*n,o*) specimen in rock. (*a*) Oral view. (*b*) Lateral view. (*c*) Aboral view. (*d*) Non-peristomial tube foot (unpaired). (*e*) Non-peristomial tube foot (paired). (*f*) Peristomial tube feet. (*g*) Oral view showing the peristome, madreporite and gonopore (peristomial tube feet omitted). (*h*) Oral view showing the madreporite and gonopore (peristomial tube feet removed). (*i*) Aboral view showing the periproct. (*j*) Lateral view showing plating in the interambulacral area containing the madreporite and gonopore (tube feet removed). Interambulacral plates are shown in green. (*k*) Oral view showing ambulacral plating at the margin of the theca (tube feet removed). (*l*) Oral view showing the internal ring (all other features transparent). (*m*) Aboral view showing ambulacral plating at the margin of the theca (tube feet removed). (*n*) Section through the theca showing the tube feet. (*o*) Section through the theca showing the internal ring. Abbreviations: cp, circular pore; go, gonopore; ir, internal ring; jp, jaw plates; ma, madreporite; pe, peristome; pr, periproct; pt, peristomial tube feet; st, small adoral non-peristomial tube foot; tf, non-peristomial tube feet; ut, unpaired non-peristomial tube feet. In *k* and *m*, perradial plates are shown in purple, adradial plates in red, and interambulacral plates in green. Scale bars: (*a–c,l*) 5 mm; (*d,e,g,k,l,n,o*) 2 mm; (*f,h,i,j,m*) 1 mm.

(figure 1*g,h*). A circlet of 16 plates (5 perradials, 10 adradials, and the plate bearing the madreporite and gonopore) surrounds the peristome.

In each ambulacral area, the plates are divided into one central column of six alternating perradial plates and two lateral columns of four adradial plates each (figure 1*k,m*). The perradial plates are broadly T-shaped and generally smaller than the adradial plates, which are L- or C-shaped. The perradial margins of the adradial plates and parts of the margins of the perradial plates flare outward to form the edges of large circular pores (figure 1*k,m*), which mark the position of the tube feet. Both the adradial and perradial plates are imbricated adorally. The pores are arranged into three slightly offset rows of two pores (figure 1*k*). There is an additional unpaired pore at the aboral end of the ambulacral area (figure 1*m*). The unpaired pore is bordered by one perradial plate and two adradial plates, the second most aboral and most adoral pores are bordered by two perradial plates and two adradial plates, and all other pores are bordered by three perradial plates and two adradial plates (figure 1*k,m*).

There are nine plated tube feet within each ambulacral area. The first pair is located within the peristome, close to the outer edge of the jaw apparatus (figure 1*a*). These peristomial tube feet are covered in tiny plates and are smaller than the other tube feet, measuring approximately 3 mm in length and 0.8 mm in diameter (figure 1*f*). The other tube feet are located outside the peristome, occurring as three slightly offset pairs, with an additional solitary tube foot at the aboral end of each ambulacral area (figure 1*a−e*). The non-peristomial tube feet increase in size aborally (reaching a maximum of approximately 14 mm in length and 2 mm in diameter), with the exception of the unpaired tube foot, which is shorter than its adoral neighbour. Within one of the ambulacral areas, the most adoral of the tube feet outside the peristome is much smaller than all others (figure 1*a*). The tube feet are preserved hollow (figure 1*n*). They consist of thin plates arranged in longitudinal rows, overlapping distally. There are at least eight rows of about 20−30 plates each in the paired tube feet (figure 1*e*) and four rows of about 13 plates each in the unpaired ones (figure 1*d*). The plates are rhomboidal to hexagonal in shape and decrease in size distally, from a maximum proximal size of approximately 0.8 mm in diameter in the paired tube feet and 1.3 mm in diameter in the unpaired tube feet; the plates of the paired tube feet are wider than the plates of the unpaired tube feet (figure 1*d,e*). The tube feet are rounded at their tips. The unpaired tube feet are preserved in a subhorizontal or gently upward curving attitude, whereas the other tube feet are curved downwards (figure 1*b*).

In all interambulacra, apart from the one that accommodates the madreporite and gonopore, there are four imbricate plates: the two adoral plates form a single column and the two aboral plates are arranged in a single row, resulting in a 1-1-2 arrangement (figure 1*k,m*). The second adoral plate is notably larger than the other three plates. In contrast, there are five imbricate plates arranged in a 1-1-2-1 pattern in the interambulacrum, accommodating the madreporite and gonopore (figure 1*j*). The most adoral plate bears the madreporite (figure 1*h,j*); the most aboral plate is the largest in this interambulacral area.

The aboral surface of the theca is composed of numerous thin, irregularly arranged imbricate plates, which are rounded to sub-hexagonal in outline and range from approximately 0.6−3 mm in diameter (figure 1*c*). Plates typically exhibit a strong granular ornament (figure 1*c,m*). The degree to which the plates overlapped one another in life is uncertain due to post-mortem collapse. The periproct is in a marginal position on the aboral surface, within the interambulacral area adjacent to that accommodating the madreporite and gonopore (figure 1*c*). It is approximately 1.7 mm in diameter and consists of several elongate triangular plates, which together form a pyramidal structure (figure 1*i*). The thecal plates surrounding the periproct are smaller than the other plates of the aboral surface.

Internally, an incomplete ring-like structure encircles the peristome (figure 1*l,o*). This structure is thin with a flattened cross-section; it is approximately 17 mm long and 7 mm wide. There is a short gap in the ring, approximately aligned with the interambulacral area where the madreporite and gonopore are located (figure 1*l*). The ring is oriented obliquely and presumably was displaced from its original horizontal position, perhaps due to partial collapse of the aboral thecal surface (figure 1*o*).

(h) Remarks

The relatively small size of the jaw apparatus and the presence of two columns of four adradial plates each and nine plated tube feet in each ambulacral area allow us to assign the Herefordshire specimen to *Sollasina* [6,11,26]. *Sollasina cthulhu* sp. nov. differs from the type species *S. woodwardi* in having: six relatively small perradial plates in a column in each ambulacral area (figure 1*k,m*) rather than three larger perradials ([6], fig. 134,2); four or five plates in each interambulacral area (figure 1*j,k,m*) rather than two ([6], fig. 134,2); and a theca that is pentagonal in outline (figure 1*a,c*) rather than rounded or elliptical ([6], fig. 134) (the exact shape in *S. woodwardi* is unclear due to post-mortem flattening). The placement of the periproct and madreporite/gonopore in adjacent interambulacral areas in *S. cthulhu* (figure 1*a,c,g*) was also reported in *S. woodwardi* [11]; this feature may be diagnostic for Sollasinidae or be characteristic of all ophiocistioids [28].

4. Results

The parsimony analysis retrieved six equally most parsimonious trees (MPTs) with a length of 86 steps, consistency index of 0.698 and retention index of 0.868 (electronic supplementary material, data S2). The strict consensus of these MPTs places *Sollasina* with the ophiocistioid *Gillocystis* as sister group to a clade comprising the ophiocistioid *Rotasaccus*, the fossil holothurian *Palaeocucumaria* and crown-group holothurians, identifying ophiocistioids as a paraphyletic assemblage of stem holothurians (figure 2*a*; electronic supplementary material, data S3). The fossil echinozoans *Bromidechinus*, *Neobothriocidaris* and *Unibothriocidaris* are more closely related to a clade of ophiocistioids, *Palaeocucumaria* and crown-group holothurians, whereas *Bothriocidaris*, *Aulechinus* and *Eothuria* are more closely related to extant echinoids. Bootstrap support values are generally low across the tree, with less than 50% support for most nodes (figure 2*a*).

The Bayesian analyses recovered very similar tree topologies to the parsimony analysis, with *Sollasina* plus *Gillocystis*
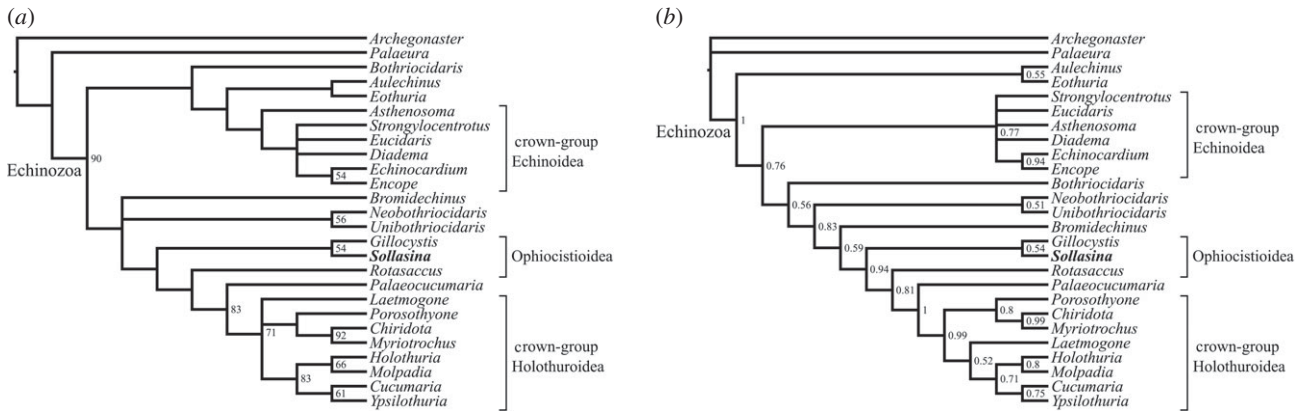
Figure 2. Phylogenetic position of ophiocistioids. (*a*) Strict consensus tree from parsimony analysis. Bootstrap support values shown for nodes with more than 50% support. (*b*) 50% majority-rule consensus tree from Bayesian analyses. Posterior probabilities shown at resolved nodes.

sister to a clade of *Rotasaccus*, *Palaeocucumaria* and crown-group holothurians in the 50% majority-rule consensus tree (figure 2*b*; electronic supplementary material, data S4). The relationships of the other fossil echinozoans are also similar to the strict consensus tree from the parsimony analysis, with the exception of *Aulechinus* and *Eothuria*, which are sister to all other echinozoans, and *Bothriocidaris*, which is sister to a clade consisting of *Neobothriocidaris*, *Unibothriocidaris*, *Bromidechinus*, ophiocistioids, *Palaeocucumaria* and crown-group holothurians. Support values are greater than 0.50 for all resolved nodes, with more than 0.70 support for most nodes (figure 2*b*).

5. Discussion

(a) Internal anatomy

An internal ring encircling the peristome (figure 1*l,o*) has not been recognized previously in any fossil echinozoan. We interpret the ring as a soft-tissue structure because it is preserved in a dark grey material optically similar to that preserving soft tissues in other echinoderms from the Herefordshire Lagerstätte [29,30]; in all these taxa, this 'dark' preservational mode is distinct from that which preserves skeletal material (figure 1*o*). A comparison with extant echinozoans suggests four possible interpretations of the internal ring: digestive tract, haemal ring, nerve ring or ring canal. It is very unlikely to be the digestive tract as there is no evidence of a connection to the mouth or anus and the small gap in the ring (figure 1*l*) is not large enough to have accommodated such connections. The haemal ring in extant echinozoans consists of a network of anastomosing lacunae [31,32], unlike the structure in *S. cthulhu* (figure 1*l*). The nerve ring and ring canal are similar in gross morphology in living echinozoans but their position differs; the nerve ring is situated inside the pyramids of the lantern in echinoids and anterior to or within the calcareous ring in holothurians, whereas the ring canal is located just above the lantern in echinoids and posterior to the calcareous ring in holothurians [31–33]. The ring in *S. cthulhu* is located above the jaw apparatus (figure 1*o*), consistent with its interpretation as the ring canal, an important part of the water vascular system hitherto unknown in fossil echinozoans.

In most extant echinozoans the ring canal gives rise to five radial canals which are connected to the tube feet by additional canals or branches of the water vascular system [31–33]; however, only the ring canal and tube feet are preserved in *S. cthulhu*. It is unclear why additional elements of the water vascular system are not preserved in our studied specimen, but their absence may relate, in part, to the unusual preservation of the Herefordshire ophiocistioid, in which most of the theca is filled with dense crystalline calcite that might have prevented preservation of soft tissues. Thus, although no radial canals are preserved in *S. cthulhu* we infer a similar organization to extant echinozoans, with five radial canals aligned with the five ambulacra. The ring canal is relatively large compared with extant echinozoans [31–33], indicating that the radial canals would have been relatively short. The tube feet may have been connected to the radial canals through additional canals or branches and large ambulacral cavities, as in modern elasipodid holothurians with greatly enlarged tube feet [34,35]. A stone canal presumably linked the ring canal to the madreporite, as in living echinoids and holothurians [31–33].

The variable curvature, imbricate plating and inconsistent orientation of the tube feet (figure 1*a–c*) indicate that they were flexible in life. The peristomial tube feet presumably played a role in feeding, manipulating food particles and conveying them to the mouth, as do the buccal podia of deposit-feeding holothurians [33]. The larger non-peristomial tube feet probably had a different function. Deep-sea elasipodid holothurians, for example, use their greatly enlarged tube feet for 'walking' [35,36]. An analogous locomotory function can be inferred for the non-peristomial tube feet in *Sollasina* and other plated ophiocistioids [6,12,37]. The gradation in length of the paired non-peristomial tube feet, which are shortest adjacent to the mouth and get longer further away (figure 1*a–c*), would have allowed all of them to make contact with the sediment surface in life, consistent with a locomotory function (figure 3). The unpaired aboral tube feet are not long enough to have reached the substrate and are preserved with tips pointing upwards (figure 1*b*), demonstrating that they were not locomotory. These tube feet might have served to right the animal if it were overturned, remove debris from the aboral surface and/or deter predators.

(b) Phylogenetic position

Our phylogenetic analyses provide strong support for the placement of ophiocistioids as stem holothurians. Both the strict consensus tree from the parsimony analysis and
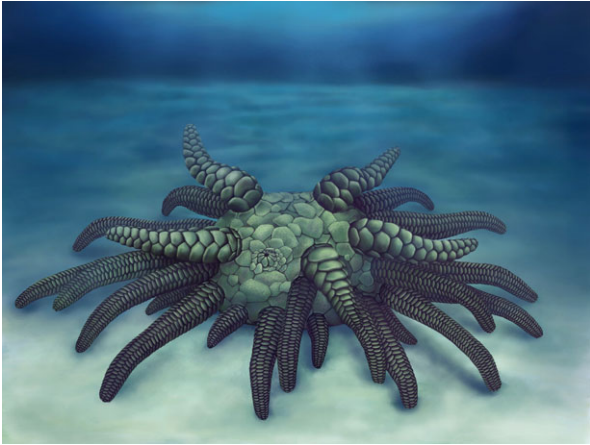
Figure 3. Reconstruction of *Sollasina cthulhu*. Courtesy of Elissa Martin, Division of Invertebrate Paleontology, Yale Peabody Museum of Natural History.

the 50% majority-rule consensus tree from the Bayesian analyses place ophiocistioids as a paraphyletic group of stem holothurians, closely related to *Palaeocucumaria* plus crown-group holothurians (figure 2). Morphological characters in our matrix (electronic supplementary material, data S1) uniting ophiocistioids and holothurians include the presence of enlarged bottom-feeding tentacles and the absence of articulated spines.

Our results agree with previous studies that identified ophiocistioids as a paraphyletic group of stem holothurians [7,18,38]. This has important implications for the assembly of the holothurian body plan. Assuming the most recent common ancestor of echinoids and holothurians had a body-wall skeleton composed of large plates, our identification of ophiocistioids as a paraphyletic group suggests that reduction of the skeleton in holothurian evolution was a stepwise process. The body-wall skeleton was reduced to rows of perradial ambulacral plates and small spicules along the branch leading to the ophiocistioid *Rotasaccus*, the fossil holothurian *Palaeocucumaria* and crown-group holothurians. Ambulacral plates were subsequently lost on the branch leading to *Palaeocucumaria* and crown-group holothurians. Finally, plated tube feet, which are present in *Palaeocucumaria*, were lost along the branch leading to crown-group holothurians. Among living echinoderms, the

expression of biomineralization genes is regulated by a suite of conserved transcription factors including *alx1* and *ets1* [39–41]. However, the number of downstream biomineralization genes and their expression during development are much lower in extant holothurians than in echinoids [42]. Thus, the reduction of the skeleton in early holothurians may have been linked to a stepwise reduction in the number and expression of these genes.

The presence of a complex jaw apparatus in both echinoids and ophiocistioids strongly suggests that this character was present in the ancestral echinozoan [43], but differences in tooth structure indicate that the teeth themselves may have evolved independently in the two classes [44]. Moreover, the probable sister-group relationship between ophiocistioids and the clade containing *Palaeocucumaria* plus crown-group holothurians (figure 2) supports the hypothesis that the holothurian calcareous ring and the echinoid jaw apparatus are homologous [7,33]. Consequently, ophiocistioids help to bridge the gap between echinoids and holothurians, two of the most morphologically divergent sister groups in the phylum Echinodermata, shedding light on the most recent common ancestor and early evolution of echinozoans.

References

1. Dunn CW, Giribet G, Edgecombe GD, Hejnol A. 2014 Animal phylogeny and its evolutionary implications. *Annu. Rev. Ecol. Evol. Syst.* **45**, 371–395. (doi:10.1146/annurev-ecolsys-120213-091627)

2. Telford MJ, Budd GE, Philippe H. 2015 Phylogenomic insights into animal evolution. *Curr. Biol.* **25**, R876–R887. (doi:10.1016/j.cub.2015.07.060)

3. Richter S, Wirkner CS. 2014 A research program for evolutionary morphology. *J. Zool. Syst. Evol. Res.* **52**, 338–350. (doi:10.1111/jzs.12061)

4. Jenner RA. 2014 Macroevolution of animal body plans: is there science after the tree? *Bioscience* **64**, 653–664. (doi:10.1093/biosci/biu099)

5. Donoghue PCJ, Purnell MA. 2009 Distinguishing heat from light in debate over controversial fossils. *Bioessays* **31**, 178–189. (doi: 10.1002/bies.200800128)

6. Ubaghs G. 1966 Ophiocistioids. In *Treatise on invertebrate paleontology, part U, Echinodermata 3 (1)* (ed. RC Moore), pp. U174–U188. Boulder, CO: Geological Society of America and University of Kansas Press.

7. Smith AB. 1984 Classification of the Echinodermata. *Palaeontology* **27**, 431–459.

8. Smith AB, Savill JJ. 2001 *Bromidechinus*, a new Ordovician echinozoan (Echinodermata), and its bearing on the early history of echinoids. *Trans. R. Soc. Edinb. Earth Sci.* **92**, 137–147. (doi:10.1017/S0263593300000109)

9. Briggs DEG, Siveter DJ, Siveter DJ. 1996 Soft-bodied fossils from a Silurian volcaniclastic deposit. *Nature* **382**, 248–250. (doi:10.1038/382248a0)

10. Briggs DEG, Siveter DJ, Siveter DJ, Sutton MD. 2008 Virtual fossils from 425 million-year-old volcanic ash. *Am. Sci.* **96**, 474–481. (doi:10.1511/2008.75.474)

11. Haude R, Langenstrassen F. 1976 *Rotasaccus dentifer* n. g. n. sp., ein devonischer Ophiocistioide (Echinodermata) mit 'holothuroiden' Wandskleriten und 'echinoidem' Kauapparat. *Paläont. Z.* **50**, 130–150.

12. Haude R. 2004 Mode of life of ophiocistioids (Echinozoa) according to plated and 'naked' forms in the Rhenish Devonian. In *Echinoderms: München*

(eds T Heinzeller, JH Nebelsick), pp. 409–416. Leiden, The Netherlands: Balkema.

13. Reich M. 2010 Evolution and diversification of ophiocistioids (Echinodermata: Echinozoa). In *Echinoderms: Durham* (eds LG Harris, SA Böttger, CW Walker, MP Lesser), pp. 51–54. Leiden, The Netherlands: CRC Press/Balkema.

14. Sutton, MD, Rahman, IA, Garwood, RJ. 2014. *Techniques for virtual palaeontology*. London, UK: John Wiley & Sons.

15. Orr PJ, Briggs DEG, Siveter DJ, Siveter DJ. 2000 Three-dimensional preservation of a non-biomineralized arthropod in concretions in Silurian volcaniclastic rocks from Herefordshire, England. *J. Geol. Soc. London* **157**, 173–186. (doi:10.1144/jgs.157.1.173)

16. Sutton MD, Garwood RJ, Siveter, DJ, Siveter DJ. 2012 SPIERS and VAXML; a software toolkit for tomographic visualisation and a format for virtual specimen interchange. *Palaeontol. Electron.* **15/5T**, 14.

17. Rahman IA, Thompson JR, Briggs DEG, Siveter DJ, Siveter DJ, Sutton MD. 2019 Data from: A new ophiocistioid with soft-tissue preservation from the Silurian Herefordshire Lagerstätte, and the evolution of the holothurian body plan. Dryad Digital Repository. (doi:10.5061/dryad.c71qf48)

18. Smith AB, Reich M. 2013 Tracing the evolution of the holothurian body plan through stem-group fossils. *Biol. J. Linn. Soc.* **109**, 670–681. (doi:10.1111/bij.12073)

19. Swofford DL. 2002 *PAUP*. Phylogenetic analysis using parsimony (*and other methods). Version 4.* Sunderland, MA: Sinauer Associates.

20. Ronquist F et al. 2012 MrBayes 3.2: efficient Bayesian phylogenetic inference and model choice across a large model space. *Syst. Biol.* **61**, 539–542. (doi:10.1093/sysbio/sys029)

21. Lewis PO. 2001 A likelihood approach to estimating phylogeny from discrete morphological character data. *Syst. Biol.* **50**, 913–925. (doi:10.1080/106351501753462876)

22. Zhang C, Rannala B, Yang Z. 2012 Robustness of compound Dirichlet priors for Bayesian inference of branch lengths. *Syst. Biol.* **61**, 779–784. (doi:10.1093/sysbio/sys030)

23. Bruguière JG. 1791 *Tableau encyclopédique et méthodique des trois règnes de la nature: contenant l'helminthologie, ou les vers infusoires, les vers intestins, les vers mollusques, &c.* Paris, France: Panckoucke.

24. Klein JT. 1734 *Naturalis dispositio echinodermatum. Accessit lucubratiuncula de aculeis echinorum marinorum, cum spicilegio de belemnitis.* Gedani [Gdańsk], Poland: Schreiber.

25. Sollas WJ. 1899 Fossils in the University Museum, Oxford: I. On Silurian Echinoidea and Ophiuroidea. *Q. J. Geol. Soc. Lond.* **55**, 692–715. (doi:10.1144/GSL.JGS.1899.055.01-04.41)

26. Fedotov DM. 1926 The plan of structure and systematic status of the Ophiocistia (Echinoderma). *Proc. Zool. Soc. Lond.* **96**, 1147–1158.

27. Lovecraft HP. 1928 The call of Cthulhu. *Weird Tales* **11**, 159–178.

28. Jell PA. 1983 Early Devonian echinoderms from Victoria (Rhombifera, Blastoidea and Ophiocistioidea). *Mem. Ass. Australas. Palaeontols.* **1**, 209–235.

29. Sutton MD, Briggs DEG, Siveter DJ, Siveter DJ, Gladwell DJ. 2005 A starfish with three-dimensionally preserved soft parts from the Silurian of England. *Proc. R. Soc. B* **272**, 1001–1006. (doi:10.1098/rspb.2004.2951)

30. Briggs DEG, Siveter DJ, Siveter DJ, Sutton MD, Rahman IA. 2017 An edrioasteroid from the Silurian Herefordshire Lagerstätte of England reveals the nature of the water vascular system in an extinct echinoderm. *Proc. R. Soc. B* **284**, 20171189. (doi:10.1098/rspb.2017.1189)

31. Ezhova OV, Ershova NA, Malakhov VV. 2017 Microscopic anatomy of the axial complex and associated structures in the sea cucumber *Chiridota laevis* Fabricius, 1780 (Echinodermata, Holothuroidea). *Zoomorphology* **136**, 205–217. (doi:10.1007/s00435-016-0341-8)

32. Ezhova OV, Malakhov VV, Egorova EA. 2018 Axial complex and associated structures of the sea urchin *Strongylocentrotus pallidus* (Sars, G.O. 1871) (Echinodermata: Echinoidea). *J. Morphol.* **279**, 792–808. (doi:10.1002/jmor.20811)

33. Hyman LH. 1955 *The invertebrates: Echinodermata.* New York, NY: McGraw-Hill.

34. Théel H. 1882 Report on the Holothuroidea dredged by H.M.S. Challenger during the years 1873–1876. Part I. Report on the scientific results of the voyage of H.M.S. Challenger during the years 1873–76 under the command of Captain George S. Nares, R.N., F.R.S. and the late Captain Frank Tourle Thompson, R.N. *Zoology* **4**, 1–176.

35. Hansen B. 1972 Photographic evidence of a unique type of walking in deep-sea holothurians. *Deep-Sea Res.* **19**, 461–462. (doi:10.1016/0011-7471(72)90056-3)

36. Gebruk A. 1995 Locomotory organs in the elasipodid holothurians: functional-morphological and evolutionary approaches. In *Echinoderm research 1995* (eds RH Emson, AB Smith, AC Campbell), pp. 95–102. Rotterdam, The Netherlands: Balkema.

37. Reich M. 2007 *Linguaserra spandeli* sp. nov. (Echinodermata: Ophiocistioidea) from the Late Permian (Zechstein) of Thuringia, Germany. *Ann. Paléontol.* **93**, 317–330. (doi:10.1016/j.annpal.2007.09.007)

38. Smith AB. 1988 Fossil evidence for the relationships of extant echinoderm classes and their times of divergence. In *Echinoderm phylogeny and evolutionary biology* (eds CRC Paul, AB Smith), pp. 85–97. Oxford, UK: Clarendon Press.

39. Gao F, Davidson EH. 2008 Transfer of a large gene regulatory apparatus to a new developmental address in echinoid evolution. *Proc. Natl Acad. Sci. USA* **105**, 6091–6096. (doi:10.1073/pnas.0801201105)

40. McCauley BS, Wright EP, Exner C, Kitazawa C, Hinman VF. 2012 Development of an embryonic skeletogenic mesenchyme lineage in a sea cucumber reveals the trajectory of change for the evolution of novel structures in echinoderms. *Evodevo* **3**, 17. (doi:10.1186/2041-9139-3-17)

41. Gao F, Thompson JR, Petsios E, Erkenbrack E, Moats RA, Bottjer DJ, Davidson EH. 2015 Juvenile skeletogenesis in anciently diverged sea urchin clades. *Dev. Biol.* **400**, 148–158. (doi:10.1016/j.ydbio.2015.01.017)

42. Zhang X et al. 2017 The sea cucumber genome provides insights into morphological evolution and visceral regeneration. *PLoS Biol.* **15**, e2003790. (doi:10.1371/journal.pbio.2003790)

43. Smith AB. 1984 *Echinoid palaeobiology.* London, UK: Allen & Unwin.

44. Reich M, Smith AB. 2009 Origins and biomechanical evolution of teeth in echinoids and their relatives. *Palaeontology* **52**, 1149–1168. (doi:10.1111/j.1475-4983.2009.00900.x)